U.P.B. Sci. Bull., Series D, Vol. 86, Iss. 4, 2024 ISSN 1454-2358

DESIGN AND RESEARCH OF AIR-SUCTION SEED METERING DEVICE FOR REGULATING THE FLAT SEEDS ADSORPTION POSTURE BY COUPLING AIR-BLOWING AND MECHANICAL

Jie ZHAO[1], Qiyun YU[2], Kexin XU[3], Zeqi LIU[4], Yulong CHEN[5*]

Aiming at the problems of poor adsorption stability of air-suction seed metering devices for flat seeds, this paper designs an air-suction seed metering device with coupled regulation of seed adsorption attitude through air blowing and mechanical compound. The experimental results show that the qualification rate is 97.99 % when the operating speed is 9.71 km/h, the airflow speed is 5.14 m/s, and the negative pressure is 3.21 kPa. The seed metering device adaptability verification test was carried out, and under the optimal parameter conditions, the qualification rate of each flat seed was greater than 97 %, which met the technical requirements of precision sowing.

Keywords: Flat Seeds; Air-suction seed metering device; Adsorption Posture; Discrete Element

1. Introduction

Precision seeding technology can reduce seedling costs and improve seedling efficiency, meeting the high efficiency, high speed, and low-cost production requirements of modern agriculture [1-3]. Seed metering device is the core equipment of precision seeding and its performance directly affects the planting effect [4,5]. Air-suction type is widely used due to its strong compatibility

[1] Shandong University of Technology, College of Agricultural Engineering and Food Science, China, Email:785574545@qq.com

[2]Shandong University of Technology, College of Agricultural Engineering and Food Science, China, Email:3228662112@qq.com

[3]Shandong University of Technology, College of Mechanical Engineering, China, Email: 2536570601@qq.com

[4]Shinva Medical Instrument Co., Ltd., China, E-mail:liuzq_67@163.com

[5*]Associate Prof., Shandong University of Technology, College of Agricultural Engineering and Food Science, China, E-mail:cyl06471@sdut.edu.cn(corresponding author)

with seed shape, small damage to seeds, and the large range of appropriate operating speeds. Currently, air-suction seed metering devices have become a research hotspot of precision seeding technology [6,7].

There are two categories of seeds according to the requirements of precision seeding: spherical seeds and flat seeds. When using air-suction seed metering devices to sow flat seeds, it is difficult to closely fit with the seed-picking pore due to their flat structure, resulting in poor adsorption stability and making it challenging to achieve high-speed precision seeding.

Celik [8] et al. compared the performance of four different types of seed metering devices for sunflowers. Yuan Yueming [9] et al. used high-speed camera technology to analyze the working process of air suction seeding of rice bud seeds. Karayel [10,11] et al. utilized three types of seed discs with different suction hole structures to sow watermelon and melon seeds for seed casting uniformity. Yazgi [12] et al. investigated operational performance and seed casting trajectory range of flat and circular maize seeds with different seed metering rates and machine inclination angles. Li Fengli [13] et al. recorded the air suction process of sunflower seeds with the help of a high-speed camera and found that the optimal adsorption posture was when the middle part of the seeds was adsorbed. The current study focuses on the mechanism of the flat seed air suction seeding performance and does not propose a regulation program for the adsorption posture of flat seeds.

This study focuses on watermelon seeds and develops an air suction seed metering apparatus to control the seed's orientation during adsorption. It introduces a combined approach involving both air propulsion and mechanical components to effectively manage the seed's position. Statistical models are created to correlate various operational metrics with their respective factors, and these models are further refined using the response surface methodology to pinpoint the most efficient design and operational settings for the seed metering equipment. Additionally, the research includes tests to validate the device's performance and assess its adaptability.

2. Materials and Methods

2.1 Structure and working principle of seed metering device

The flat seed metering device, its structure mainly consists of seed covering, seeding discs, air blowing device, a negative pressure shell, air blowing interface, inclined boss as in Fig. 1. Seed covering additional air blowing interface as the positive pressure air flow blowing interface constitutes the key structure of air-suction seed metering device to regulate the adsorption posture. The seeding discs are equipped with an inclined boss at the seeding pores to form an inclined boss seeding discs, which is the key structure for mechanical control of the adsorption posture.

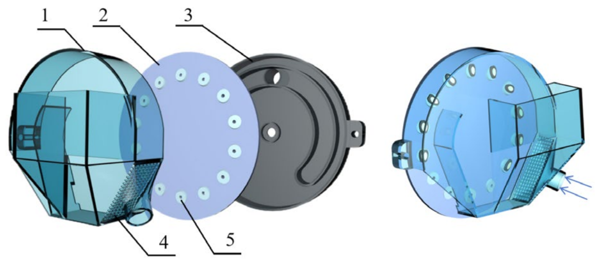

Fig. 1. The schematic diagram of the seed metering device. 1. seed covering, 2. seeding discs, 3. negative pressure shell, 4. air-blowing interface, 5. inclined boss

The work of seed metering device can be divided into three stages: seed filling, seed carrying, and seed discharge. The fan supplies the negative pressure chamber with a pressure differential, forming a negative pressure air flow at the seed-taking hole. The positive pressure fan carries out air-blowing disturbance to the seeds. The seeds reach the ideal adsorption posture under the synergistic effect of air-blowing disturbance, inclined boss, and suction hole adsorption force. The seeds are not easy to fall and change posture when adsorbed on the inclined boss in the seed group. The seeds fall under their gravity to complete a seed metering when they rotate to the area where the air is isolated by an air-blocking device.

The diameter of the seeding discs for normal air-suction seed metering devices is 140-260 mm. In this study, considering the requirements for sowing large-size watermelon seeds, the diameter of the seeding discs is selected to be 245 mm. The diameter of the suction hole has a greater impact on the seed-filling performance of the seed metering device. Because of the large difference in variety size, the suction hole diameter of the seed discharging device is 4-7 mm. Considering that parallel between flat seeds and the surface of suction holes is the optimal adsorption posture, and the distance between suction holes ensures that seeds have enough space for regulation under the premise of airflow disturbance, the diameter of suction holes is set at 5 mm in this paper. To ensure that the distance between two adjacent suction holes in the seeding discs is greater than the longest size of a seed, the number of suction holes is 14.

2.2 Inclined boss structure and parameter design

The structure of the inclined boss directly affects the seeding performance of the seeding discs. Therefore, it was needed to perform parameter design for the structure of the inclined boss. It was determined the size of the diameter of the boss and the tilting direction to match air blowing structure to disturb the seeds and design the tilting angle to enhance the overturning ability of the seed punching process of the watermelon. As shown in Fig. 2, the key parameters of the inclined boss include the radius r_1 of the bottom of the boss, the height h_1 of the boss, the inclination angle α_1 of the boss, and the inclination angle β_1 of the bottom of the boss.

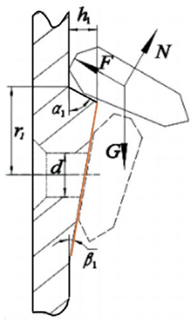

Fig. 2. Structure diagram of inclined convex

For the seed to slide smoothly into the suction hole, the inclined boss should have enough disturbing capacity that be satisfied:

$$\begin{cases} G\cos\alpha_1 \geq F \\ F = \mu N \\ N = G\sin\alpha_1 \end{cases} \tag{1}$$

G is seed gravity, N; F is the friction force of the boss ramp to the seed, N; N is the support force of the boss ramp to the seed, N; μ is the friction coefficient between the seed and the boss ramp.

Organized:

$$\alpha_1 \leq arctan\frac{1}{\mu} \tag{2}$$

From Eq. 2, get $\alpha_1 \leq 60.26$ ° and take $\alpha_1 = 60$ °, $\mu = 1.73$. To ensure that the inclined boss can enable the seed to slide and the overlap range between the flattened surface of the seed and the surface of the boss after sliding can contain suction holes, it should be satisfied:

$$\begin{cases} h_1 < \dfrac{c_{\min}}{2} \\ l_{\max} \le \dfrac{2r_1 \tan\alpha_1 - h_1}{\cos\beta_1 \tan\alpha_1} \le 2w_{\min} \\ \dfrac{2r_1 \tan\alpha_1 - h_1 + d\tan\alpha_1}{2\cos\beta_1 \tan\alpha_1} < b_{\min} \end{cases} \tag{3}$$

According to the calculation of the size of the watermelon seed, get the height of the camber $h_1 < 2$ mm, the bottom radius of the camber r_1 takes the value range of 9-11 mm, the camber downward inclination angle β_1 takes the value range of 5-15 °, take the h_1 is 1.5 mm, r_1 is 10 mm, β_1 is 10 °.

Air-suction seeding discs suck the seeds and detach them from the seed group in working. Airflow field at the suction hole is crucial for the seeding performance. The force of the seeds under the composite effect of air blowing disturbing the flow field and negative pressure adsorbing flow field is explored [14,15].

The force analysis of the seeding discs seed filling is shown in Fig. 3.

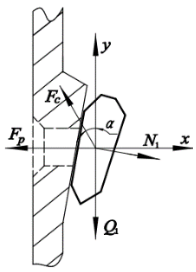

Fig. 3. Seed force analysis

When filling the seeds, to make the seeds adsorbed on the suction holes do not fall off during the synchronized rotation with the seeding discs,
it is necessary to meet:

$$\begin{cases} \left(F_p + F_c \sin\alpha - N_1 \cos\beta_1\right) \cdot \frac{d}{2} \ge \left(Q_1 - F_c \cos\alpha\right) \cdot \frac{c}{2} \\ F_p = P_1 \cdot F_1 \\ S_1 = \pi \left(\frac{d}{2\cos\beta_1}\right)^2 \end{cases} \tag{4}$$

Where F_p is the suction pore adsorption force, N; F_c is air blowing pressure, N; N_1 is the support force given to the seeds by the slanting surface of the boss during the seed filling process, N; Q_1 is the combined force of gravity, centrifugal force and inter-seed friction on the seeds during the seed filling process, N, and P_1 is the pressure in the negative pressure chamber, Pa.

Organized:

$$P_1 \geq \frac{\left[\left(Q_1 - F_c \cos\alpha\right)\cdot c - F_c \sin\alpha d + N_1 \cos\beta_1 d\right]\cdot 4\cos\beta_1}{\pi d^3} \quad (5)$$

From Eq. 5, it can be seen that when F_c becomes bigger, P_1 becomes smaller, and airflow disturbance can effectively reduce the negative pressure of seed filling.

2.3 Geometric parameters of flattened seeds

Typical flat seeds (watermelon) were selected as the research object. Four varieties of watermelon seeds, namely, Inner Mongolia large watermelon seeds, Inner Mongolia middle watermelon seeds, and Lanzhou big melon seeds, were used in the market; Randomly selected 100 seeds of each variety, the use of vernier calipers were to measure the seed length l, width w, and thickness c, take the average value of the statistics of its data in Fig. 4.

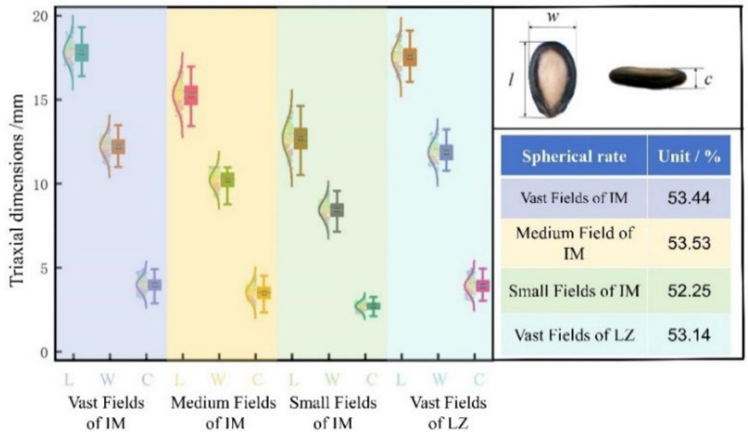

Fig. 4. Seed dimensions analysis

From the above results, it can be seen that the characteristics of the Lanzhou big board are the most representative, so the subsequent simulation and rack experiments chose Lanzhou plate as the experimental object.

2.4 Bench experiment

Air-blowing disturbance feeding and tilted boss seeding discs combination together, installed in the JPS-12 type seeding performance test bench for a bench test, test seed selection "Lanzhou big plate" watermelon seeds, its thousand-grain weight of 321.57 g, water content of 7.1 %.

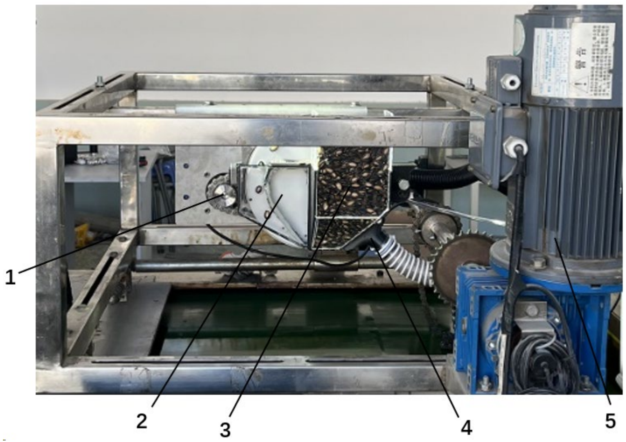

Fig. 5. Seed metering device test bench. 1. motor, 2. seed metering device, 3. watermelon seeds, 4. air-blowing interface, 5. ventilator.

The test method refers to GB/T 6973-2005 Test Methods for Single Grain (Precision) seed metering devices, 251 seeds were collected in each group of tests, and the test was repeated three times. The test results were averaged, and the qualified rate and missing rate were used as the evaluation indexes of seeding performance [16]. Combined with the results of the pre-experiment, the test factors were selected as operating speed, airflow speed, and negative pressure, and obtain the optimal parameters of the three factors, the principle of Box-Behnken experimental design was adopted, and the levels of the test factors are shown in Table 1.

$$\begin{cases} S = \frac{n_1}{N} \times 100\% \\ M = \frac{n_2}{N} \times 100\% \\ D = \frac{n_3}{N} \times 100\% \end{cases} \tag{6}$$

S is the single particle adsorption rate, %; *M* is the reabsorption rate, %; *D* is the leakage rate, %; n_1 is the number of suction pores for adsorbing a single seed; n_2 is the number of suction pores for adsorbing multiple seeds; n_3 is the number of adsorption pores for unabsorbed seeds; *N* is the statistical number of suction holes.

Table 1

Test factors and levels

Level	Test factor		
	Operating speed, km/h	Airflow velocity, m/s	Negative pressure, kPa
1	8	4	2
2	10	5	3
3	12	6	4

3. Experimental Results and Discussion

3.1 Analysis of bench experiment results

The bench test results are shown in Table 2.

Table 2

Test scheme and results

Test serial number	Test factor			Test index	
	Operating speed X_1, km/h	Airflow velocity X_2, m/s	Negative pressure X_3, kPa	Qualified rate Y_1, %	Missing Rate Y_2, %
1	8	4	3	95.06	1.36
2	12	4	3	96.97	1.88
3	8	6	3	96.67	1.24
4	12	6	3	93.58	1.15
5	8	5	2	95.54	1.83
6	12	5	2	95.15	2.38
7	8	5	4	96.53	1.42
8	12	5	4	95.63	1.73
9	10	4	2	96.32	1.63
10	10	6	2	95.23	1.43
11	10	4	4	96.13	1.35
12	10	6	4	96.28	0.92
13	10	5	3	97.92	0.71
14	10	5	3	98.13	0.82

15	10	5	3	97.86	0.61
16	10	5	3	98.22	0.76
17	10	5	3	97.77	0.74

The experimental data in Table 2 were analyzed using Design-Expert 13.0 software to derive the regression models of pass rate and missing rate with operating speed, airflow rate, and negative pressure, eliminating the factors that were not significant to the regression model viz:

$$\begin{cases} Y_1 = 97.98 - 0.31X_1 - 0.34X_2 + 0.29X_2 - 1.25X_1X_2 + 0.31X_2X_3 - 1.34X_1^2 - 1.07X_2^2 - 0.92X_3^2 \\ Y_2 = 0.76 + 0.16X_1 - 0.18X_2 - 0.23X_3 - 0.15X_1X_2 + 0.60X_1^2 + 0.52X_3^2 \end{cases} \tag{7}$$

The ANOVA of the regression model was analyzed to get Table 3, the regression model of qualified rate and missed seeding rate was highly significant ($P < 0.01$), the lack of fit was not significant ($P > 0.05$), and the regression model fit the actual seeding situation realistically. Through the P value analysis, it was concluded that the primary and secondary order of the influence of the three factors on qualified rate was airflow speed, operation speed, and negative pressure, and the primary and secondary order of the influence on the missed seeding rate was negative pressure, airflow speed, and operation speed.

Table 3

Regression model analysis of variance

Variance source	Qualified rate Y_1				Missing rate Y_2			
	Sum of squares	Degree of freedom	F	P	Sum of squares	Degree of freedom	F	P
Model	26.86	9	75.04	< 0.0001**	3.88	9	48.58	< 0.0001**
X_1	0.76	1	19.17	0.0032**	0.21	1	23.43	0.00019**
X_2	0.92	1	23.25	0.0019**	0.27	1	30.84	0.0009**
X_3	0.68	1	17.06	0.0044**	0.43	1	48.18	0.0002**
X_1X_2	6.25	1	155.13	< 0.0001**	0.093	1	10.48	0.0143*
X_1X_3	0.065	1	1.63	0.2418	0.014	1	1.62	0.2435
X_2X_3	0.38	1	9.66	0.0171*	0.013	1	1.49	0.2618
X_{12}	7.60	1	191.15	< 0.0001**	1.48	1	167.03	< 0.0001**

X_{22}	4.79	1	120.35	< 0.0001**	0.031	1	3.15	0.1033
X_{32}	3.59	1	90.33	< 0.0001**	1.13	1	127.48	< 0.0001**
Residual error	0.28	7			0.062	7		
Misfit term	0.14	3	1.28	0.3956	0.038	3	2.14	0.2383
Pure error	0.14	4			0.024	4		
Sum	27.14	16			3.94	16		

Note: $P < 0.01$ (highly significant, **); $P < 0.05$ (significant, *)

To study the effect of each interaction factor on the single seed rate and breakage rate, the response surface plots of each interaction factor on the single grain rate and breakage rate are plotted, as shown in Fig. 6 and Fig. 7.

Fig. 6a shows that when negative pressure is 3 kPa and the fixed airflow speed is constant, the qualified rate increases and then decreases with the increase of operating speed; when the fixed operating speed is constant, the qualified rate also increases and then decreases with the increase of airflow speed. When the operating speed is 9-11 km/h and airflow velocity is 4.5-5.5 m/s, the qualified rate is relatively high. Fig. 6b shows that when airflow speed is 5 m/s and the fixed negative pressure is unchanged, the passing rate increases and then decreases with the increase of operating speed; when the fixed operating speed is unchanged, the passing rate also increases and then decreases with the increase of negative pressure. When the operating speed is 9-11 km/h and negative pressure is 2.5-3.5 m/s, the passing rate is relatively high. Fig. 6c shows that when the operating speed is 10 m/s and the fixed negative pressure is unchanged, the qualification rate increases and then decreases with the increase of airflow speed; when the fixed airflow is unchanged, the qualification rate also increases and then decreases with the increase of negative pressure. When air velocity is 4.5-5.5 m/s and negative pressure is 2.5-3.5 m/s, the qualification rate is relatively high. Fig. 7a shows that when negative pressure is 3 kPa and the fixed airflow speed is constant, the missing rate decreases and then increases with the increase of operating speed; when the fixed operating speed is constant, the missing rate also decreases and then increases with the increase of airflow speed. When the operating speed is 9-11 km/h and airflow velocity is 4.5-5.5 m/s, the missing rate is relatively low.

Fig. 7b shows that when airflow speed is 5 m/s, fixed negative pressure is constant, missing rate decreases and then increases with the increase of operating speed; fixed operating speed is constant, with the increase of negative pressure, missing rate also decreases and then increases. When the operating speed is 9-11 km/h and negative pressure is 2.5-3.5 m/s, the missing rate is relatively low. Fig. 7c shows that when the operating speed is 10 m/s and the fixed negative pressure is unchanged. the missing rate shows a trend of decreasing and then increasing with the increase of airflow speed; when the fixed airflow is unchanged, the missing rate also shows a trend of decreasing and then increasing with the increase of negative pressure. When air velocity is 4.5-5.5 m/s and negative pressure is 2.5-3.5 m/s, the missing rate is relatively low.

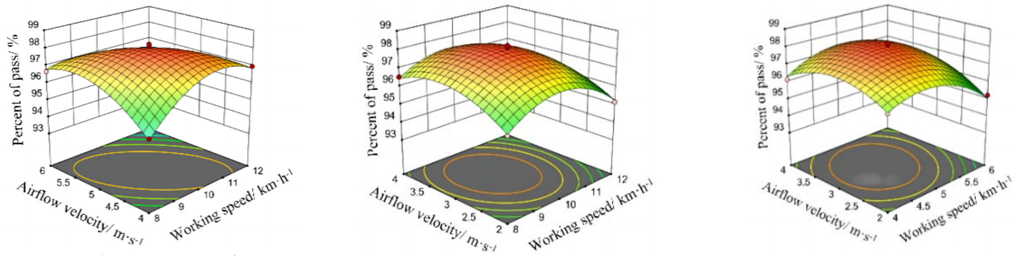

a.Y_1（X_1， X_2， 0） b.Y_1（X_1， 0， X_3） c.Y_1（0， X_2， X_3，）

Fig. 6. Influence of factor interaction on qualification rate

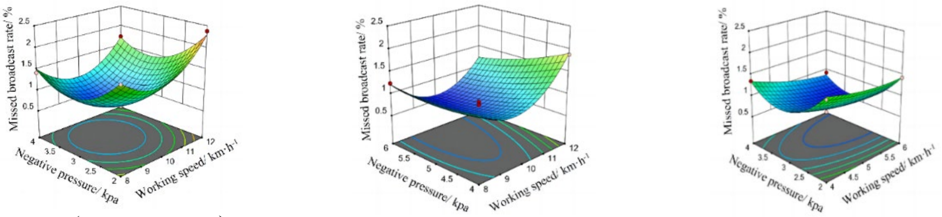

a. Y1（X1，X2，0） b. Y1（X1，0，X3） c. Y1（0，X2，X3，）

Fig.7. Influence of factors interaction on missing rate

3.2 Parameter optimization and verification

To combine the working parameters of air-suction seed metering device based on air-blowing disturbance feeding, the objective function and constraint conditions are established by using the optimization module of Design-Expert software, taking the maximum qualified rate and the minimum missing rate as evaluation indexes:

$$\begin{cases} max\, Y_1 \\ max\, Y_2 \\ s.t. \begin{cases} 8 \leq X_1 \leq 12 \\ 4 \leq X_2 \leq 6 \\ 2 \leq X_3 \leq 3 \end{cases} \end{cases} \quad (8)$$

Through parameter optimization, our team concluded that when the operation speed is 9.71 km/h, airflow velocity is 5.14 m/s, and negative pressure is 3.21 kPa, operation performance is the best meanwhile the qualified rate is 97.99 % and the missing rate is 0.67 %.

Table 4

Seeding suitability test results

breed	Test indicators	
	Pass rate , %	leakage rate , %
Lanzhou big board	98.16	0.53
Inner Mongolia Big piece	97.85	0.68
Inner Mongolia Medium piece	97.61	0.74
Inner Mongolia small piece	97.43	0.46

To verify the accuracy of optimization results and the adaptability of the seed metering device to different flat seeds, our team conducted three repeated tests when operation speed was 9.71 km/h, airflow velocity was 5.14 m/s, and negative pressure was 3.21 kPa. The test results are shown in Table 4. Under the optimal parameters, the qualified rate of each flat seed is more than 97 %, and the missing rate is less than 1 %. It is consistent with the optimized results and the technical requirements for precision seeding.

4. Conclusions

(1) To improve the control of the suction posture of the seed metering device to the flat seed and to improve the seed-taking performance, this air-suction seed metering device regulates the flat seed adsorption posture by coupling air-blowing and mechanical. The structure of this device was designed to determine that the diameter of seed discs was 245 mm, the diameter of the suction hole was 5 mm and the number of suction holes was 14. Boss bottom radius r_1 is 10 mm, boss height h_1

is 1.5 mm, boss inclination angle α_1 is 60 °and boss lower inclination angle β_1 is 10 °.

(2) Through simulating and verifying the working performance of the incline boss structure, it is determined that its disturbance ability to seeds is far greater than that of grooved seed metering and flat discs.

(3) The primary and secondary order of the influence on the qualified rate is airflow speed, operating speed and negative pressure, on the missing rate is negative pressure airflow speed and operating speed. When the operating speed is 9.71 km/h, airflow speed is 5.14 m/s and negative pressure is 3.21 kPa, the qualified rate is 97.99 %, and the missing rate is 0.67 %. When the operating speed is 9.71 km/h, airflow speed is 5.14 km/h and negative pressure is 3.21 kPa, the qualified rate is 97.99 %, and the missing rate is 0.67 %.

(4) The suitability test of the seed metering device was carried out. Under the optimal parameters, the qualified rate of each flat seed was more than 97 %, and the missing rate was less than 1 %. It is consistent with the optimized results and the technical requirements of precision seeding.

REFERENCES

[1]. *Rajaiah P, Mani I, Parray R A, et al.* Design and development of precision planter for paddy direct seeding [J]. Journal of Agricultural Engineering, 2020, 57(4): 302-314.

[2]. *Mhasaye V A, Patil C V.* Design and Development of Manually Operated Cotton Seed Planter [J]. JETIR, 2019, 6(4): 199-206-199-206.

[3]. *Rui Liu, Liu Zhongjun, Zhao Jiale, et al.* Optimization and Experiment of a Disturbance-Assisted Seed Filling High-Speed Vacuum seed-metering device Based on DEM-CFD [J]. Agriculture, 2022, 12(9).

[4]. *Li Ding, Yang Li, Liu Shourong et al.* Design of air suction high-speed precision seed-metering device for corn with auxiliary seed filling tray [J]. Journal of Agricultural Engineering, 2018, 34 (22): 1-11.

[5]. *Jinwu Wang, Qi Xin, Xu Changsu, et al.* Design Evaluation and Performance Analysis of the Inside-Filling Air-Assisted High-Speed Precision Maize seed-metering device [J]. Sustainability, 2021, 13(10).

[6]. *Javidan S M, Mohamadzamani D.* Design, construction, and evaluation of automated seed-metering device with ultrasonic sensors for row detection [J]. Journal of Biosystems Engineering, 2021: 1-10.

[7]. *Wei, Ji Ruiqi, He Xiaoning, et al.* Research on high-speed precision seed-metering device for peanuts with driven combined trough-assisted air-suction seed attachment [J]. Journal of Agricultural Machinery, 2023, 54(05): 59-70.

[8]. *Celik A., I. Ozturk, T. R-Way.* Effects of Various Planters on Emergence and Seed Distribution Uniformity of Sunflower [J]. Applied Engineering in Agriculture, 2007, 23(1).

[9]. *Yuan Yueming, Ma Xu, Zhu Yanhua et al.* Seeding with air suction seed-metering device based on high-speed camera technology [J]. Journal of Jilin Agricultural University, 2008, (04): 617-620.

[10]. *Özmerzi Aziz, Davut Karayel.* Effect of Forward Speed on Hill Dropping Uniformity of a Precision Vacuum seed-metering device [J]. HortTechnology, 2004, 14(3).

[11]. *Davut Karayel, Güngör Orhan, Šarauskis Egidijus.* Estimation of Optimum Vacuum Pressure of Air-Suction seed-metering device of Precision seed-metering devices Using Artificial Neural Network Models [J]. Agronomy, 2022, 12(7).

[12]. *Yazgi A , Navid H , Weckler P ,et al.* Performance Modeling and Seed Releasing Characteristics of a Corn Planter Metering Unit Using Response Surface Methodology [J]. Applied Engineering in Agriculture, 2015, 33(2): 181-189.

[13]. *Li Fengli, Zhao Manquan, Liu Fei et al.* Work of air suction seed-metering device and seed movement [J]. Agricultural Mechanization Research, 2018, 40 (01): 150-154.

[14]. *Peng Xinyi.* Design and experiment of pneumatic guide rail peanut precision seed-metering device [D]. Shihezi University, 2022.

[15]. *Yan Jianwei, Wei Song, Hu Dongjun et al*. Design and experiment of air suction roller seed-metering device for white radish [J]. Agricultural Mechanization Research, 2023, 45 (11): 1-174.

[16]. *Madhusudan B S, Preetham M*. Design, development and performance evaluation of manually operated groundnut planter [J]. Indian Journal of Ecology, 2020, 47(3): 858-862.